Cancer Cell
Article

# Coordinated Regulation of Polycomb Group Complexes through microRNAs in Cancer

Qi Cao,[1,2] Ram-Shankar Mani,[1,2] Bushra Ateeq,[1,2] Saravana M. Dhanasekaran,[1,2] Irfan A. Asangani,[1,2] John R. Prensner,[1,2] Jung H. Kim,[1,2] J. Chad Brenner,[1,2] Xiaojun Jing,[1,2] Xuhong Cao,[1,3] Rui Wang,[1,2] Yong Li,[1,2] Arun Dahiya,[1] Lei Wang,[1,2] Mithil Pandhi,[1] Robert J. Lonigro,[1,2] Yi-Mi Wu,[1,2] Scott A. Tomlins,[1,2] Nallasivam Palanisamy,[1,2,6] Zhaohui Qin,[7] Jindan Yu,[1,2,9] Christopher A. Maher,[1,2,4] Sooryanarayana Varambally,[1,2,6,8] and Arul M. Chinnaiyan[1,2,3,5,6,8,*]
[1]Michigan Center for Translational Pathology
[2]Department of Pathology, University of Michigan
[3]Howard Hughes Medical Institute, University of Michigan Medical School
[4]Center for Computational Medicine and Bioinformatics
[5]Department of Urology, University of Michigan
[6]Comprehensive Cancer Center, University of Michigan Medical School
Ann Arbor, MI 48109, USA
[7]Department of Biostatistics and Bioinformatics, Center for Comprehensive Informatics, Emory University, Atlanta, GA 30329, USA
[8]These authors contributed equally to this work
[9]Present address: Division of Hematology/Oncology, Northwestern University, Robert H. Lurie Comprehensive Cancer Center, Chicago, IL 60611, USA
*Correspondence: arul@umich.edu
DOI 10.1016/j.ccr.2011.06.016

## SUMMARY

**Polycomb Repressive Complexes (PRC1 and PRC2)-mediated epigenetic regulation is critical for maintaining cellular homeostasis. Members of Polycomb Group (PcG) proteins including EZH2, a PRC2 component, are upregulated in various cancer types, implicating their role in tumorigenesis. Here, we have identified several microRNAs (miRNAs) that are repressed by EZH2. These miRNAs, in turn, regulate the expression of PRC1 proteins BMI1 and RING2. We found that ectopic overexpression of EZH2-regulated miRNAs attenuated cancer cell growth and invasiveness, and abrogated cancer stem cell properties. Importantly, expression analysis revealed an inverse correlation between miRNA and PRC protein levels in cell culture and prostate cancer tissues. Taken together, our data have uncovered a coordinate regulation of PRC1 and PRC2 activities that is mediated by miRNAs.**

## INTRODUCTION

Polycomb group (PcG) proteins are evolutionarily conserved regulators of gene silencing important in metazoan development (Surface et al., 2010), stem cell pluripotency (Pereira et al., 2010), and X chromosome inactivation (Cao et al., 2002; Margueron and Reinberg, 2011). PcG proteins form multiprotein repressive complexes called PRCs. Both PRC1 and PRC2 play a critical role in the maintenance of normal and cancer stem cell populations (Ezhkova et al., 2009; Lukacs et al., 2010; Pietersen et al., 2008). Dysregulation of PcG proteins can contribute to a number of human diseases, most notably, cancer (Bracken and Helin, 2009; Margueron and Reinberg, 2011).

Key components of the human PRC2 include the histone methyltransferase Enhancer of Zeste Homolog 2 (EZH2), and its binding partners, Embryonic Ectoderm Development (EED) and Suppressor of Zeste 12 (SUZ12), which function as a multisubunit complex that trimethylates histone H3K27. PRC2 is thought to be recruited to target genomic loci by long noncoding RNAs (ncRNAs) such as HOTAIR (Gupta et al., 2010; Kaneko et al., 2010; Rinn et al., 2007). EZH2, which is the enzymatic component of PRC2, is elevated in aggressive forms of prostate

### Significance

Polycomb group (PcG) proteins are chromatin-modifying complexes that regulate epigenetic silencing and play an important role in determining cell fate. PcG proteins form two major complexes, Polycomb Repressive Complex 1 (PRC1) and Polycomb Repressive Complex 2 (PRC2). PRC2 methylates histone H3 on lysine27 (H3K27), a chromatin mark that stimulates PRC1 to enact gene silencing at target genes. Employing in vitro and in vivo cancer models and human tumor studies, we demonstrate that PRC2 and PRC1 coordinate their functions through regulation of specific microRNAs. Increased PRC2 activity in cancer leads to repression of these microRNAs, and subsequent increase of PRC1 components. Thus, we propose that key microRNAs link PRC2 to PRC1 forming an integral regulatory axis of the epigenetic silencing machinery.

and breast cancer (Kleer et al., 2003; Varambally et al., 2002), as well as multiple other solid tumors (Matsukawa et al., 2006; Sudo et al., 2005). Loss of microRNA (miRNA)-101, has been shown to be one mechanism that leads to elevated EZH2 and PRC2 activity in tumors (Cao et al., 2010; Chiang et al., 2010; Friedman et al., 2009; Varambally et al., 2008; Wang et al., 2010). Also, miR-26a was reported to target EZH2 in cancer and myogenesis (Lu et al., 2011; Wong and Tellam, 2008). Accumulating evidence suggests that increased activity of PRC2 is oncogenic as measured by cell proliferation (Bracken et al., 2003; Varambally et al., 2002), cell invasion (Cao et al., 2008; Kleer et al., 2003), anchorage-independent growth (Bracken et al., 2003; Kleer et al., 2003), maintenance of tumor-initiating cells, tumor xenograft growth (Yu et al., 2007b), and metastasis in vivo (Min et al., 2010) .

A key collaborator of PRC2 in epigenetic silencing is human PRC1, which comprises B lymphoma Mo-MLV insertion region 1 (BMI1), RING1 (also known as RING1A or RNF1) and RING2 (also known as RING1B or RNF2), and functions as a multiprotein complex to ubiquitinate histone H2A at lysine 119 (uH2A) (Cao et al., 2005; Wang et al., 2004). The prevailing hypothesis is that PRC2-mediated trimethylation of H3K27 recruits PRC1 to gene loci, which enacts chromatin condensation and epigenetic silencing of target genes (Bracken and Helin, 2009). Like PRC2 component EZH2, BMI1 and RING2 have been shown to be elevated in a number of tumor types (Glinsky et al., 2005; Sánchez-Beato et al., 2006) and regulate self-renewal of embryonic stem cells and cancer stem cells (Galmozzi et al., 2006; Valk-Lingbeek et al., 2004). The mechanism of how PRC2 and PRC1 coordinate their functions is still unclear. In this study, we sought to explore the regulatory axis between PRCs and whether miRNAs mediate the synergy between the two complexes.

## RESULTS

### PcG Proteins Are Regulated by miRNAs

Previously, it has been reported that EZH2, the methyltransferase subunit of the PRC2 complex, is repressed by miR-101 (Friedman et al., 2009; Varambally et al., 2008) and miR-26a (Lu et al., 2011; Wong and Tellam, 2008). We hypothesized that PcG proteins (comprising the mammalian PRC complexes) may in general be regulated by miRNAs. To test this hypothesis, we knocked down Dicer, a key protein required for miRNA processing, by employing Dicer-specific siRNA duplexes. By immunoblot analysis, we found that PRC2 proteins EZH2, EED, and SUZ12, and PRC1 proteins BMI1 and RING2 were increased significantly by three different Dicer siRNA duplexes (Figure 1A; see Figure S1A available online). These experiments support the general notion that miRNAs function to repress PcG expression.

### Identification of EZH2-Regulated miRNAs

To explore miRNAs regulated by PRC2 globally, we knocked down EZH2 in DU145 prostate cancer cells with a validated siRNA targeting EZH2 and monitored miRNA expression with Illumina BeadChips. In parallel, we compared these miRNA profiles with DU145 cells relative to four benign epithelial cell lines of either prostate (PrEC and RWPE) or breast (H16N2 and HME) origin. We primarily observed miRNAs that were decreased in cancer cells relative to benign that are targets of repression by EZH2, and thus PRC2. We found 63 miRNAs that were downregulated in DU145 cells compared with the normal cell lines, and inhibition of EZH2 by knockdown restored expression of these miRNAs (Figure 1B; Table S1). Similarly, the expression levels of these 63 miRNAs were downregulated in breast cancer cells BT-549 and SKBr3 compared with breast benign epithelial cells H16N2 and HME (Figure 1B; Table S1) Using miRNA target analysis (www.targetscan.org), we identified 14 miRNAs as top candidates with the following properties: (1) upregulated by EZH2 knockdown in DU145 cancer cells which express high levels of PRC2; (2) higher in benign cell lines compared with DU145 cells, and (3) predicted to bind to the 3′ untranslated region (UTR) of target PRC1 components based on TargetScan (Figure 1C). Thirteen of the 14 miRNAs meeting these criterion fell into several known miRNAs clusters and families, including miR-200b and miR-200c in the miR-200 family, which has previously been reported to repress BMI1 (Shimono et al., 2009; Wellner et al., 2009). Of the 14 miRNAs, only miR-203, which is also known to target BMI1 (Wellner et al., 2009), does not belong to any known cluster or family (Figure S1B).

### EZH2-Regulated microRNAs Inhibit Expression of PRC1 Proteins BMI1 and RING2

To pinpoint the specific miRNAs that target PRC1 (out of the 14 that were nominated by computational approaches) (Figure 1C), we overexpressed each of them in BT-549 and DU145 cancer cell lines and monitored EZH2, BMI1, and RING2 protein expression (Figure 2A; Figure S2A). Of these, miR-181a, b decreased RING2 protein levels, miR-203 decreased BMI1 protein levels while miR-200b,c decreased both BMI1 and RING2 (Figure 2A). Attenuation of these PRC1 members resulted in decreased global ubiquityl-H2A, a known PRC1 substrate and mark of gene repression. Furthermore, PRC1 targets including p16INK4A (Jacobs et al., 1999a) and p21 (Waf1/Cip) (Fasano et al., 2007) were derepressed (Figure 2A). Several of the miRNAs computationally predicted to inhibit PRC1 failed to do so by overexpression including miR-17, miR-19b, and others (Figure S2A). Similar to protein levels, real-time qPCR showed miR-181a,b and miR-200b,c decreased RING2 transcript levels and miR-200b,c and miR-203 decreased BMI1 transcript levels in BT-549 cells (Figure 2B). As expected, overexpressing miR-200b or miR-203 decreased BMI1 occupancy on known PRC1 target gene p16, p19 (Jacobs et al., 1999b), p21, and HoxC13 (Cao et al., 2005) regions (Figure S2B).

To further corroborate our miRNA overexpression studies, we also extinguished expression of miRNAs using antagomiRs (Krützfeldt et al., 2005). Consistent with our predictions, antagomiR-200b, antagomiR-200c, and antagomiR-203 increased BMI1 protein levels, while antagomiR-181a, antagomiR-181b, antagomiR-200b, and antagomiR-200c increased RING2 protein levels in H16N2 cells (Figure 2C).

To evaluate whether these miRNAs directly bind to the 3′ UTR of BMI1 or RING2, we cloned the predicted binding sites of the wild-type or mutant 3′ UTR into a luciferase reporter system and cotransfected them with miRNA expression vectors into BT-549 cells (Figure 2D; Figures S2C–S2F). As expected, inhibition of luciferase activity was observed in cells transfected with constructs containing wild-type binding sites but not the mutant

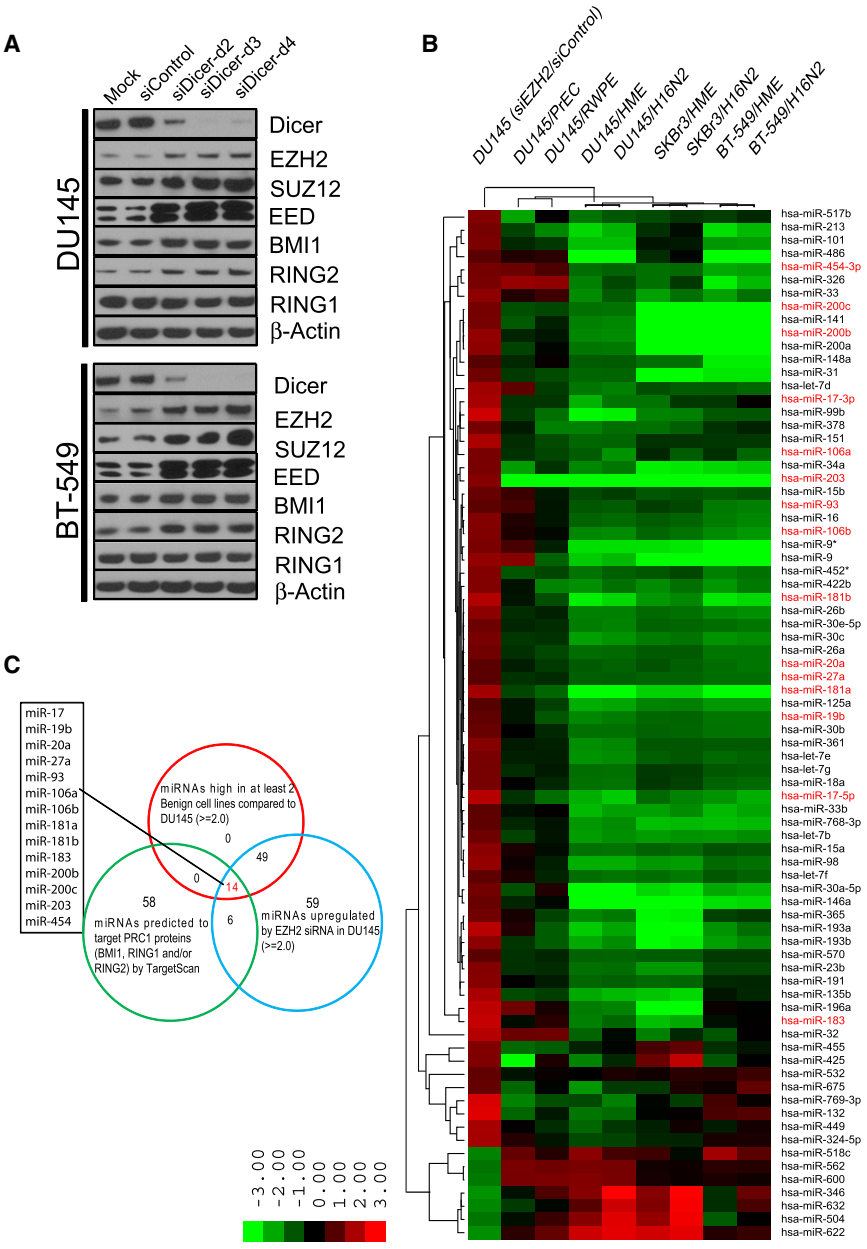


**Figure 1. PcG Proteins Are Regulated by miRNAs**

(A) Knockdown of Dicer in DU145 and BT-549 cells by three different Dicer-specific duplexes and PcG protein expression was assessed.

(B) miRNA profiling of DU145 prostate cancer cells in which EZH2 was knocked down compared with DU145 cancer cells relative to benign cells HME, PrEC, RWPE, and H16N2. Shades of red represent increased gene expression while shades of green represent decreased expression.

(C) A Venn diagram depicting 14 miRNAs that were upregulated by EZH2 knockdown, had high endogenous levels in normal cells, and were predicted to target PRC1 proteins.

See also Figure S1 and Table S1.

constructs. The RING2 3′ UTR reporters were downregulated by miR-181a, miR-181b, miR-200b, and miR-200c while the BMI1 3′ UTR reporters were downregulated by miR-200b, miR-200c, and miR-203 (Figure 2D).

We next determined whether the miRNAs that regulate PRC1 were directly regulated by PRC2 in BT-549 and DU145 cells. Cells were transfected with either a validated EZH2 siRNA or miR-101 (both of which target and downregulate the PRC2), and expression levels of target miRNAs were measured by real-time PCR. miR-181a, miR-181b, miR-200a, miR-200b, miR-200c, and miR-203 expression levels were increased in EZH2 siRNA or miR-101-transfected cells. Expression of miRNAs miR-217 and miR-219, two control microRNAs not predicted to be regulated by EZH2, were not altered (Figure 3A).

Further, we observed similar expression changes in these microRNAs upon stable overexpression of miR-101 or EZH2 shRNA in DU145 and SKBr3 cells (Figure S3A). Also we observed that miR-101 was increased in DU145 cells in which EZH2 was stably knocked down, suggesting the existence of feedback regulation between EZH2 and miR-101. In contrast, overexpression of EZH2, but not EZH2ΔSET (which is missing its catalytic SET domain), decreased miR-181a, miR-181b, miR-200a, miR-200b, miR-200c, and miR-203 levels in H16N2 cells (Figure S3B).

Next, we treated DU145 cells with the global histone methylation inhibitor, deazaneplanocin A (DZNep), that depletes PRC2 and thus attenuates H3K27me3 (Tan et al., 2007). Interestingly, DZNep treatment led to derepression of the putative PRC2-targeted miRNAs including miR−181a,b, miR-200a,b,c, and miR-203 (Figure 3B). This effect was both concentration and incubation time dependent. Control microRNAs, miR-217, miR-219, and miR-21 were not affected by DZNep treatment.

In addition to DZNep, we evaluated other chemical inhibitors of epigenetic pathways. As HDAC activity is essential for EZH2 function (Cao et al., 2008; Kleer et al., 2003), and EZH2 directly or indirectly facilitates DNA methylation (Viré et al., 2006), we predicted that treatment with the HDAC inhibitor suberoylanilide hydroxamic acid (SAHA) and/or the DNA methylation inhibitor 5-aza-2′-deoxycytidine (5-aza-dC) would inhibit EZH2-mediated epigenetic modifications, leading to an increase in miRNA expression. Treatment of BT-549 and DU145 cells with 5-aza-dC or SAHA alone or in combination, resulted in a marked increase in miR-181a,b, miR-200a,b,c, and miR-203 expression, suggesting epigenetic regulation of these microRNAs (Figure 3C).

Importantly, when we overexpressed EZH2 by adenovirus in DZNep or SAHA and 5-aza-dC-treated DU145 cells, EZH2 could

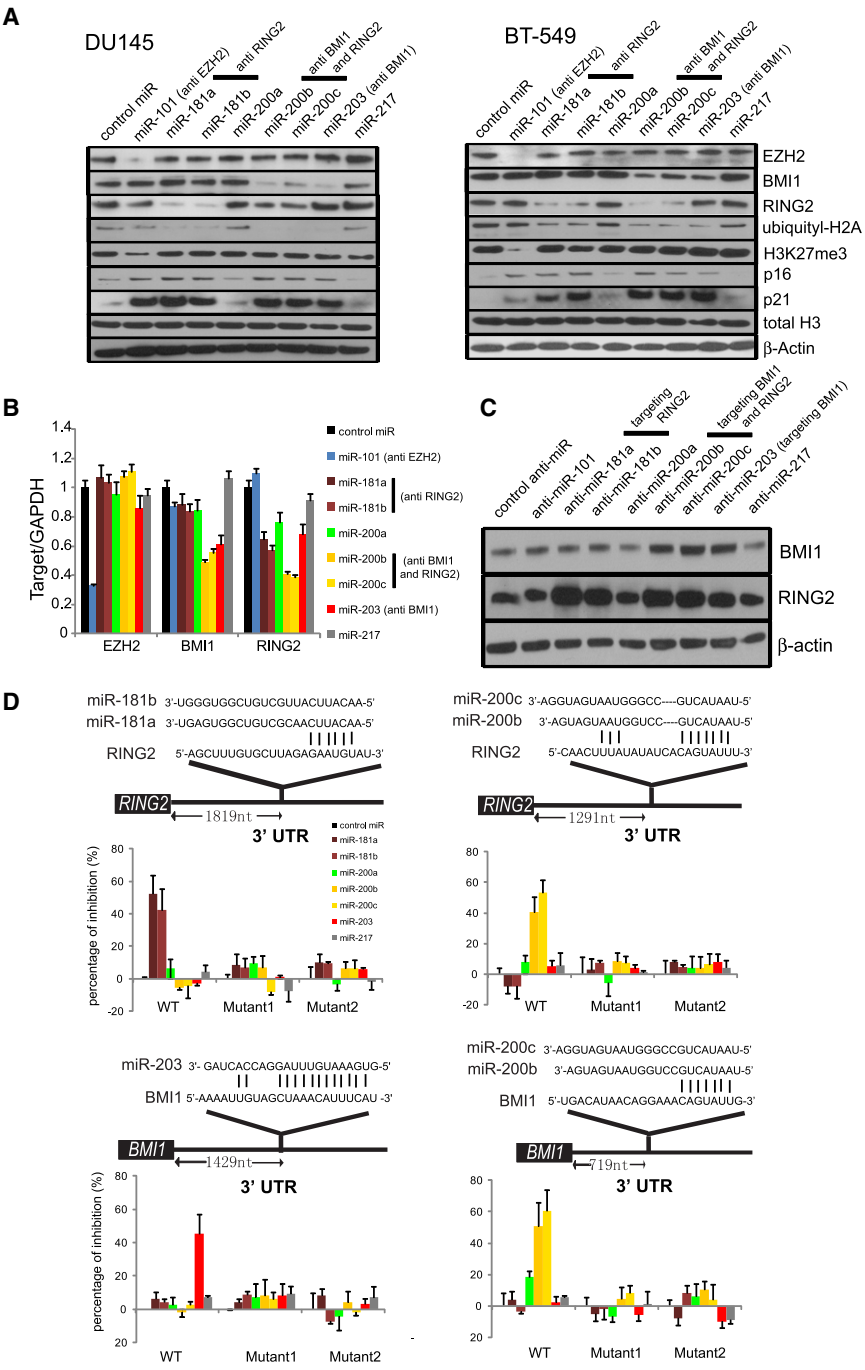


**Figure 2. PRC2-Regulated miRNAs Repress PRC1 Proteins BMI1 and RING2**

(A) Overexpression of indicated miRs in DU145 and BT-549 cells and expression of PRC components, PRC2 histone mark H3K27me3, PRC1 target histone mark ubiquityl-H2A and indicated genes by immunoblot analysis. β-actin and total H3 were used as loading controls.

(B) As in (A), except transcript level was assessed in BT-549 by qPCR.

(C) Transfection of indicated antagomiRs (anti-miR) in H16N2 cells and immunoblot analysis for BMI1 and RING2. β-actin was used as a loading control.

(D) TargetScan analysis depicting potential binding sites for EZH2-regulated miRNAs in the 3′ UTR of BMI1 and RING2. Luciferase reporter assays with wild-type or mutant 3′ UTR constructs of BMI1 or RING2 demonstrate that miR-181a, miR-181b, miR-200b, miR-200c, and miR-203 repress BMI1 and/or RING2 activity.

All bar graphs are shown with ± SEM. See also Figure S2.

completely abolish DZNep-mediated miRNA upregulation (Figure S3C), and partially decreased SAHA and 5-aza-dC-mediated miRNA upregulation (Figure S3D) presumably because SAHA and 5-aza-dC also inhibited HDAC and DNMT activities.

To confirm that EZH2 regulates these microRNAs by epigenetic repression, we performed chromatin immunoprecipitation (ChIP) assays with anti-H3K27me3, EZH2 and BMI1 antibodies in BT-549 cells. Interestingly, H3K27me3 and EZH2 occupied the PRC2-regulated miRNAs regions as expected. In addition, BMI1 also occupied these regions (Figure S3E), suggesting that a negative feedback system between PRC2-regulated miRNAs and PRC1 may exist. Furthermore, an EZH2-specific siRNA (Figure S3F) or treatment with 5-aza-dC and SAHA, either alone or in combination (Figure 3D), markedly decreased the H3K27me3 occupancy in these regions.

## EZH2-Regulated miRNAs Attenuate Growth, Invasiveness, and Self-Renewal of Cancer Cells

Because EZH2 has been shown to repress several tumor suppressor genes (Cao et al., 2008; Chen et al., 2005; Fujii et al., 2008; Min et al., 2010; Yu et al., 2007b, 2010), we postulated that the EZH2-regulated microRNAs also functioned as tumor suppressors. Consistent with this hypothesis, overexpression of either miR-181a, miR-181b, miR-200a, miR-200b, miR-200c, or miR-203 markedly attenuated BT-549 and DU145 cell proliferation to levels similar to that of cells transfected with EZH2 siRNA, or cells overexpressing miR-101 (Figure 4A *p < 0.001, **p < 0.01; Figure S4A). Likewise, overexpression of either miR-181a, miR-181b, miR-200a, miR-200b, miR-200c, or miR-203 inhibited the in vitro invasive potential of BT-549 and DU145 cells through modified Boyden chambers coated with Matrigel (Figure 4B, *p < 0.005, **p < 0.02). However, overexpressing EZH2-repressed miRNAs had no effect on the invasiveness of RWPE-UBE2L3-KRAS and RWPE-SLC45A3-BRAF stable cells, in which fusion proteins UBE2L3-KRAS (Wang et al., 2011) and SLC45A3-BRAF (Bonci et al., 2008; Palanisamy et al., 2010) confer neoplastic properties to RWPE cells

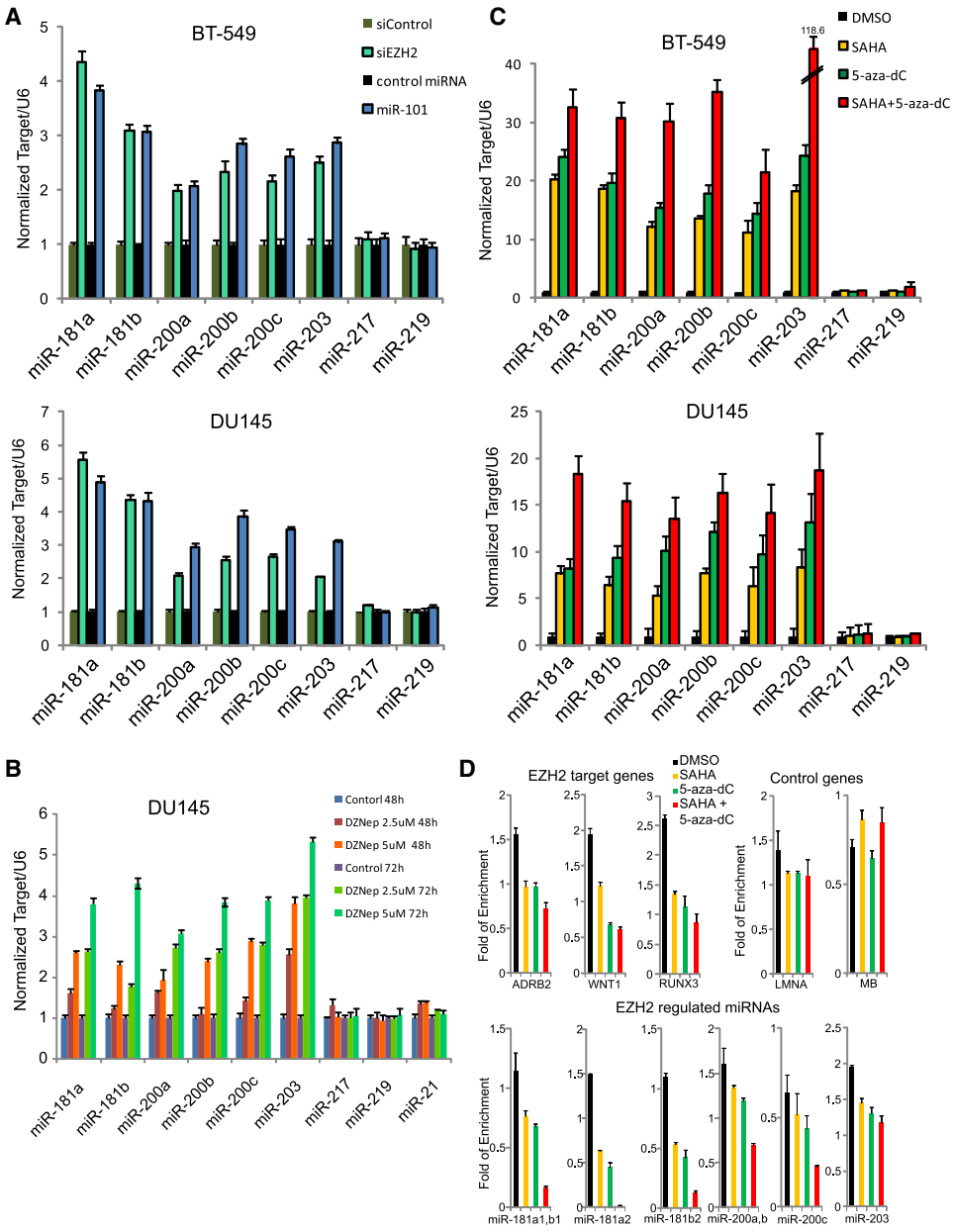


**Figure 3. PRC2 Silences Multiple miRNAs by Epigenetic Mechanisms**

(A) Taqman miRNA qPCR analysis of indicated miRs in BT-549 and DU145 cells in which EZH2 was knocked down using siRNA or miR-101 (a microRNA which targets EZH2). Quantitative microRNA levels were normalized against U6.

(B) As in (A), except DZNep at two different doses and time points was incubated with DU145 cells.

(C) As in (A), except SAHA and/or 5-aza-dC was used in BT-549 and DU145 cells.

(D) ChIP-qPCR analysis of H3K27me3 at indicated genes and microRNAs in BT-549 cells treated with SAHA and/or 5-aza-dC.

All bar graphs are shown with ± SEM. See also Figure S3.

(Figure S4B), suggesting that EZH2-repressed miRNAs miR-181a,b, miR-200b,c, and miR-203 may inhibit cell invasion through acting on PRC1 proteins. However, EZH2-repressed miRNAs still decreased RWPE-UBE2L3-KRAS and RWPE-SLC45A3-BRAF proliferation (Figure S4C), consistent with a critical role of PcG proteins in cell growth.

To investigate whether miR-181a, miR-181b, miR-200a, miR-200b, miR-200c, or miR-203 inhibit anchorage-independent growth, we performed soft agar colony formation assays. Similar to miR-101 and EZH2 knockdown controls, overexpression of miR-181a, miR-181b, miR-200a, miR-200b, miR-200c, and miR-203 markedly suppressed DU145 colony formation (Figure 4C, *$p < 0.001$, **$p < 0.01$). Next, we evaluated the ability of DU145 to form prostatospheres in sphere-promoting cell media. This assay serves as a surrogate measure of stem cell-like phenotypes, and cells that are able to form spheres have

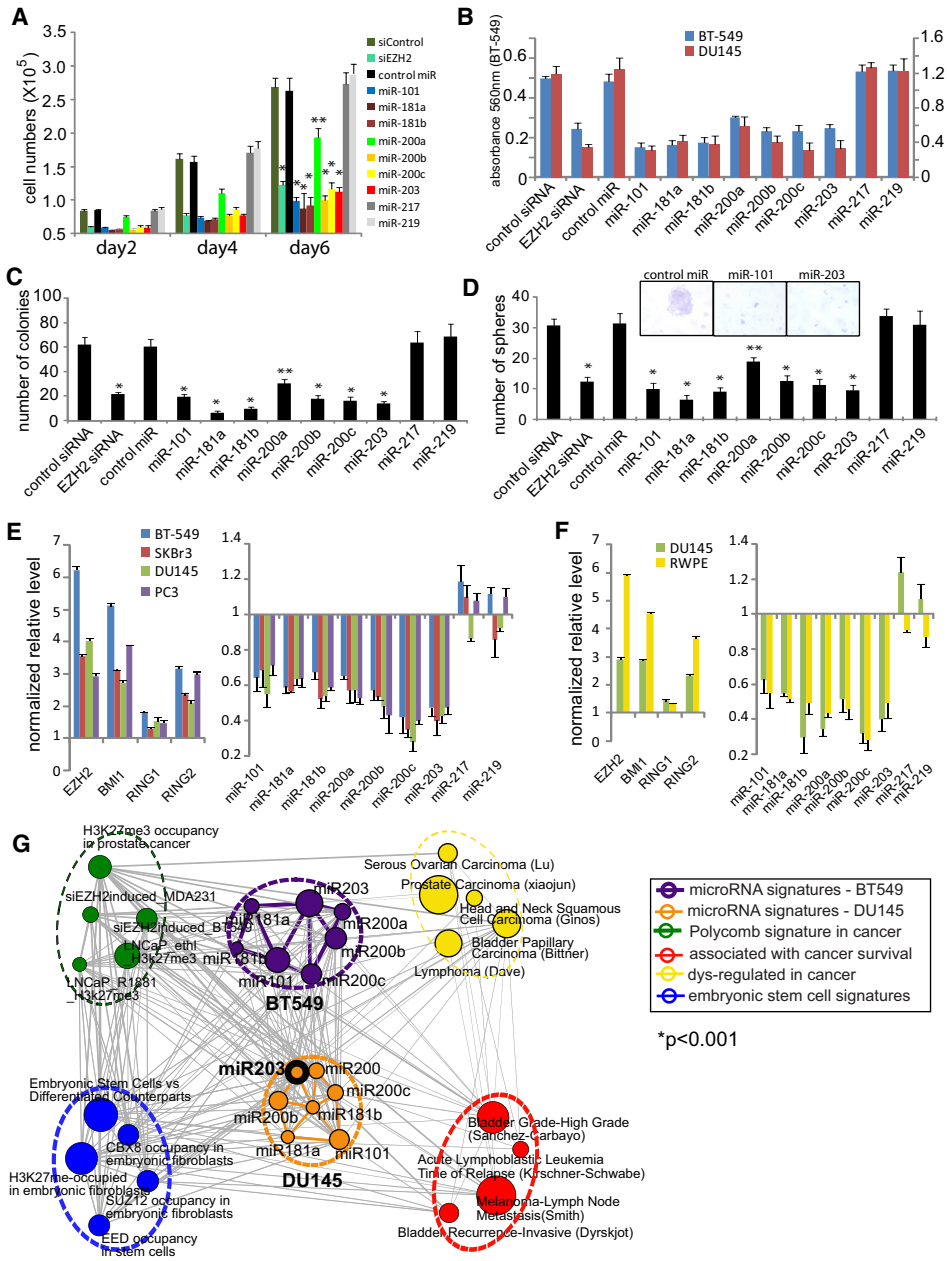


**Figure 4. PRC2-Mediated Regulation of microRNAs Potentiates the Cancer Cell Phenotype**

(A) Overexpression of PRC2-regulated miRNAs, but not control miR-217 or miR-219, inhibited BT-549 cell proliferation. EZH2 siRNA and miR-101 overexpression were positive controls and miR-217 and miR-219 overexpression were negative controls. *$p < 0.001$, **$p < 0.01$. (Student's t test).

(B) Overexpression of PRC2-regulated miRNAs decreased BT-549 and DU145 cell invasion in vitro. *$p < 0.01$. (Student's t test).

(C) Overexpression of PRC2-regulated miRNAs suppressed DU145 anchorage-independent growth in soft agar. *$p < 0.01$. (Student's t test).

(D) Overexpression of EZH2-regulated miRNAs decreased prostatosphere formation by DU145 cells. *$p < 0.01$. (Student's t test). Representative images of prostatospheres (scale bar: 100 μm) were shown in the inset.

(E) qPCR analysis demonstrating EZH2, BMI1 and RING2 transcript levels were higher in spheres compared with monolayer culture, while miR-101, miR-181a,b, miR-200a,b,c, and miR-203, but not miR-217 or miR-219, were lower in spheres compared with monolayers. Expression level of each gene was normalized to GAPDH or U6 and normalized to corresponding monolayer cultured cell line.

(F) qPCR analysis showing EZH2, BMI1 and RING2 levels were higher in sorted CD24-/CD44+ DU145 and RWPE cells compared with the unsorted population, while miR-101, miR-181a,b, miR-200a,b,c, and miR-203, but not miR-217 or miR-219, were lower in CD24-/CD44+ DU145 and RWPE cells compared with an unsorted population.

(G) Genes regulated by EZH2-repressed miRNAs cluster into multiple functional concepts. BT-549 and DU145 cells were transfected with EZH2-repressed miRNAs followed by gene expression profiling and Molecular Concepts analysis. Each node represents a molecular concept or set of biologically related genes. miR-101, miR-181a, miR-181b, miR-200a, miR-200b, miR-200c, and miR-203 (miRNA signatures, purple for BT-549, orange for DU145) were enriched

enhanced stem cell characteristics (Lawson et al., 2007). We found that miR-181a, miR-181b, miR-200a, miR-200b, miR-200c, and miR-203 overexpression, as well as miR-101 overexpression and EZH2 siRNA controls, significantly inhibited the ability of DU145 cells to form spheres in this assay (Figure 4D, *$p < 0.001$, **$p < 0.01$). Intriguingly, several genes implicated in pluripotency and cellular reprogramming by induced pluripotency, such as Klf4, Sox2, and c-Myc, were markedly downregulated by miR-200b, miR-200c, and miR-203, and marginally decreased by miR-101, miR-181a, miR-181b, and miR-200a expression, but not by miR-217 or miR-219 controls (Figure S4D). Relative to the human embryonic stem cell H7, BT-549 and DU145 cancer cells have comparable expression levels of iPS factors and PcG proteins (Figure S4E).

Next, we measured expression levels of EZH2, BMI1, RING2, and key microRNAs relevant to this study in spheres and monolayers. In BT-549, SKBr3, DU145, and PC3 cells, we observed that EZH2, BMI1, and RING2 levels were higher in spheres than in monolayers; conversely miR-101, miR-181a, miR-181b, miR-200a, miR-200b, miR-200c, and miR-203 levels were lower in spheres than in monolayers (Figure 4E). Using DU145 and RWPE parental cell lines, we employed flow cytometry to isolate cells with high expression of the CD44 surface antigen and low expression of the CD24 surface antigen (CD24-/CD44+), a cell population enriched for stem cell-like phenotypes (Hurt et al., 2008). We measured EZH2, BMI1, RING2, and miRNA levels in CD24-/CD44+ cells compared with total, unsorted cells. We observed that EZH2, BMI1, and RING2 levels were increased in CD24-/CD44+ cells, but miR-101, miR-181a, miR-181b, miR-200a, miR-200b, miR-200c, and miR-203 expression were decreased in this cell population (Figure 4F). Taken together, the data provide compelling evidence for the coordinated regulation of PRC2, PRC1, and miRNAs in the maintenance of a differentiated cellular state and inhibition of stem cell-like phenotypes.

In order to understand the functional biology of the miRNAs identified in this study, we sought to identify global gene expression patterns and molecular pathways to which they might contribute. We conducted gene expression microarray analyses of DU145 and BT-549 cells transfected with control miRNA, miR-101, miR-181a, miR-181b, miR-200a, miR-200b, miR-200c, or miR-203. As shown in Table S2 and Table S3, EZH2-repressed miRNAs targeted many predicted genes. When we analyzed the miRNA-regulated genes using Molecular Concepts Maps (MCM) (Tomlins et al., 2007b), as expected, molecular concepts associated with these miRNAs were highly overlapping, showing a high correlation to gene sets representing multiple cancers, metastatic cancer processes, cancer survival, Polycomb Group targets, and stem cell-related genes (Figure 4G; Table S4).

In order to further examine the molecular link between PRC1 and PRC2 activities, we generated DU145 cells stably overexpressing miR-200b and miR-203 (Figure S5A) and monitored levels of BMI1 and RING2. BMI1 and RING2 were decreased in miR-200b stable cells while only BMI1 was decreased in miR-203 stable cells. In addition, uH2A, the histone modification mediated by PRC1, was similarly decreased in both miR-200b- and miR-203-expressing cells. Interestingly, BMI1, RING2, and uH2A, as well as EZH2 and H3K27me3, were decreased in miR-101 stable expressing DU145 cells (Figure 5A) suggesting that prolonged knockdown of PRC2 components leads to suppression of PRC1. Using cell count and Boyden chamber invasion assays, we found that similar to miR-101, miR-200b and miR-203 stably expressing cells grew more slowly and were less invasive than vector-transfected cells (Figures 5B and 5C). Intriguingly, coexpression of BMI1 or EZH2 (control) without the 3′ UTR both restored the proliferation and invasion properties of DU145 cells despite the presence of miR-101, miR-200b, or miR-203 (Figures 5B and 5C). Importantly, murine xenograft experiments demonstrated that DU145 cells with stable knockdown of PRC1 proteins BMI1 or RING2 (Figure S5B), or expressing miR-181b (Figure S5C), miR-200b, or miR-203 grew more slowly than the vector control in vivo ($p = 0.0001$, Figures 5D and 5E).

### EZH2-Regulated miRNAs Inversely Correlate with PRC Protein Levels in Prostate Cancer

Since miR-101, miR-181a, miR-181b, miR-200a, miR-200b, miR-200c, and miR-203 appear to play an important role in cancer progression, we next measured the endogenous expression levels of these miRNAs by qPCR analysis of a cohort of benign prostate, localized, and metastatic prostate cancers in which we had measured miR-101, miR-217, and EZH2 levels previously (Varambally et al., 2008). As expected, miR-181a, miR-181b, miR-200a, miR-200b, miR-200c, and miR-203 levels were lowest in metastatic prostate cancer tissues, and highest in benign prostate tissues (Figure 6A). In addition, immunoblot analyses showed that BMI1, RING2, and uH2A, as well as EZH2, but not RING1, were increased in metastatic prostate cancer compared with benign tissues and localized cancer samples (Figure 6B; Figure S6A). EZH2 levels were highly correlated with BMI1, RING2, and H2A protein levels (Figure S6B), further supporting a molecular link between PRC1 and PRC2 expression and activities during cancer progression. As expected, ChIP assays showed that H3K27me3-marked chromatin occupied the miR-203 upstream region in metastatic prostate cancer, but not in localized prostate cancer (PCA) (Figure S6C). Similarly, DNA methylation of the miR-203 genomic region was observed in localized and metastatic prostate cancer but not benign prostate tissue (Figure 6C). Taken together, these data suggest that EZH2-mediated epigenetic repression of miR-181a, miR-181b, miR-200b, miR-200c, and miR-203 results in an upregulation of PRC1 proteins BMI1 and RING2 and histone code ubiquityl-H2A in advanced prostate cancer.

## DISCUSSION

This study unravels the intricacies in the regulation of the polycomb protein complexes mediated by various miRNAs, and substantiates the essential role played by PRC in cancer. We demonstrated that increased PRC2 activity results in repression of numerous miRNAs that are known to be important in the

for concepts related to cancer (yellow), cancer survival (red), stem cell likeness (blue), and function of polycomb group (green). All bar graphs are shown with ±SEM.
See also Figure S4, and Table S2, Table S3, and Table S4.

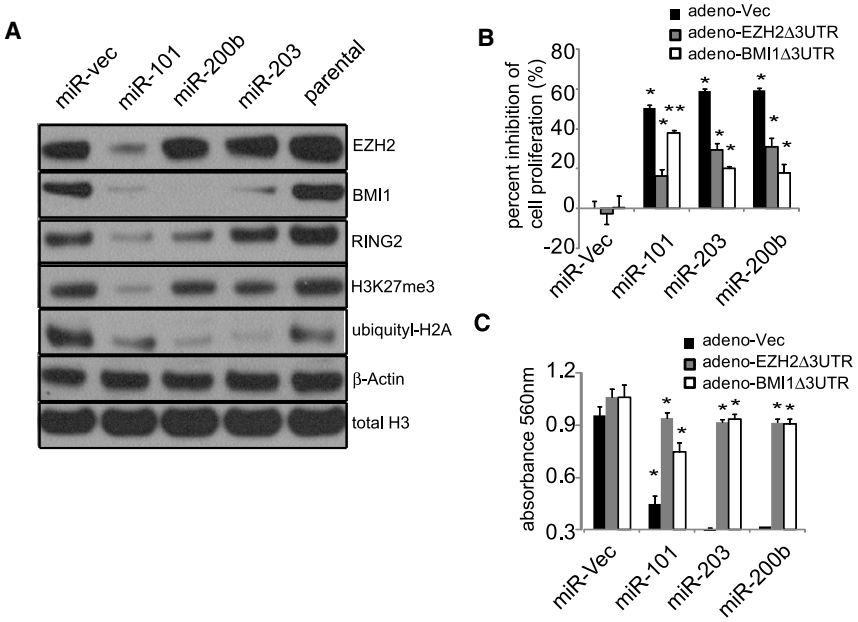


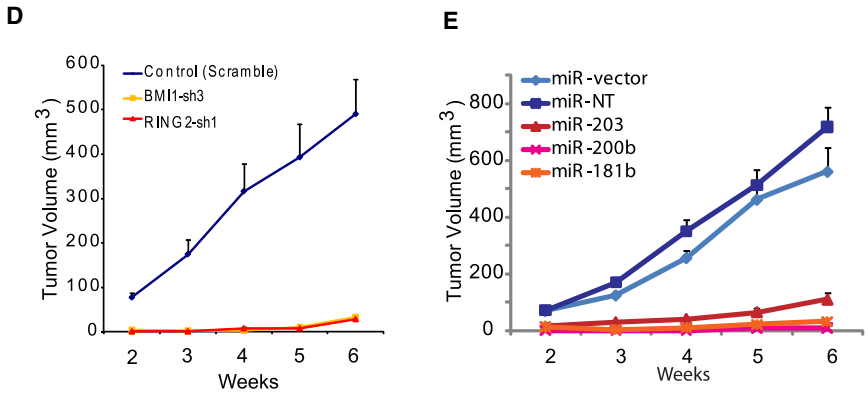


**Figure 5. PRC2-Repressed miRNAs Inhibit Tumor Growth**

(A) DU145 cells stably overexpressing miR-101, miR-200b, and miR-203 demonstrated repression of EZH2, BMI1, or RING2, as well as decreased H3K27me3 and ubiquityl-H2A (uH2A) levels.

(B and C) Coexpression of EZH2Δ3′UTR or BMI1Δ3′UTR rescued cell proliferation (B), and invasiveness (C) of DU145 cells stably overexpressing miR-101, miR-203, or miR-200b.

(D) Stably knocking down BMI1 or RING2 by BMI1-specific shRNA (BMI1-sh3) or RING2-specific shRNA (RING2-sh1) decreased DU145 tumor growth in mice. N = 8 for DU145 control (scramble), BMI1-sh3, and RING2-sh1, respectively, were used for the xenograft.

(E) Stable overexpression of miR-181b, miR-200b, or miR-203 decreased DU145 tumor growth in mice. DU145 miR-vector (N = 9), miR-NT (nontargeting) (N = 8), miR-181b (N = 8), miR-200b (N = 8), or miR-203 (N = 7) were used for the xenograft experiment. DU145 stable pools were injected subcutaneously.

All bar graphs are shown with ± SEM. See also Figure S5.

maintenance of stem cell-like phenotypes in cancer cells. We show that PRC2 epigenetically represses miR-181a, miR-181b, miR-200b, miR-200c, and miR-203 expression by facilitating H3K27me3 trimethylation at these loci, and that exogenous overexpression of miR-181a, miR-181b, miR-200b, miR-200c, and miR-203 inhibits a cancer phenotype in vitro. Furthermore, miR-181b, miR-200b, and miR-203 overexpression suppressed prostate tumor formation and growth in mouse xenografts. Recently, several groups have also reported roles for miR-200b, miR-200c, and miR-203 in controlling stem cell differentiation (Yi et al., 2008), epithelial-to-mesenchymal transition (EMT) (Park et al., 2008; Wellner et al., 2009), and cancer progression (Faber et al., 2008; Shimono et al., 2009).

Here, we demonstrated that PRC1 proteins BMI1 and RING2 are direct targets of miR-181a, miR-181b, miR-200b, miR-200c, and miR-203 in breast and prostate cancer. Furthermore, we observed a significant negative correlation between PRC2 expression and miR-181a, miR-181b, miR-200b, miR-200c, and miR-203, as well as a strong positive correlation between EZH2, BMI1, and RING2 protein levels. Intriguingly, earlier studies suggested a discrepancy between BMI1 protein and RNA levels in prostate tissues, as protein levels were increased while RNA levels were decreased during prostate cancer progression (Varambally et al., 2005). It is possible that regulation of PRC proteins occurs at both transcriptional and posttranscriptional levels by separate mechanisms. We provide evidence that EZH2-regulated microRNAs contribute to the maintenance of a differentiated cellular state, and that miR-181a, miR-181b, miR-200b, miR-200c, and miR-203 function as tumor suppressors during prostate cancer progression.

Interestingly, several recent studies have reported similar microRNA-protein regulatory networks that play critical roles in cancer. In one study, the *RAS* proto-oncogene was shown to be coordinately regulated by the *let-7* family of miRs (Johnson et al., 2005). Likewise, the miR-15a–miR-16-1 cluster, located on chr13q14, was proposed to serve as a tumor suppressor in prostate tissue by regulating levels of cancer-related genes such as BCL2, CCND1, and WNT3A (Bonci et al., 2008). Recently, Poliseno et al. (2010) reported a proto-oncogenic miRNA-dependent network in prostate cancer progression in which the miR-106b∼25 cluster regulates PTEN expression and cooperates with MCM7 in cellular transformation. These studies, along with our present study, strongly suggest that dysregulation of miRNA and target protein networks may contribute to cancer development.

Here, we propose a model for a coordinated PRC2-PRC1 oncoprotein axis, and epigenetic link between H3K27me3 and ubiquityl-H2A, mediated by PRC2-regulated miRNAs (Figure 7). Recently, Iliopoulos et al. (2010) reported that miR-200b

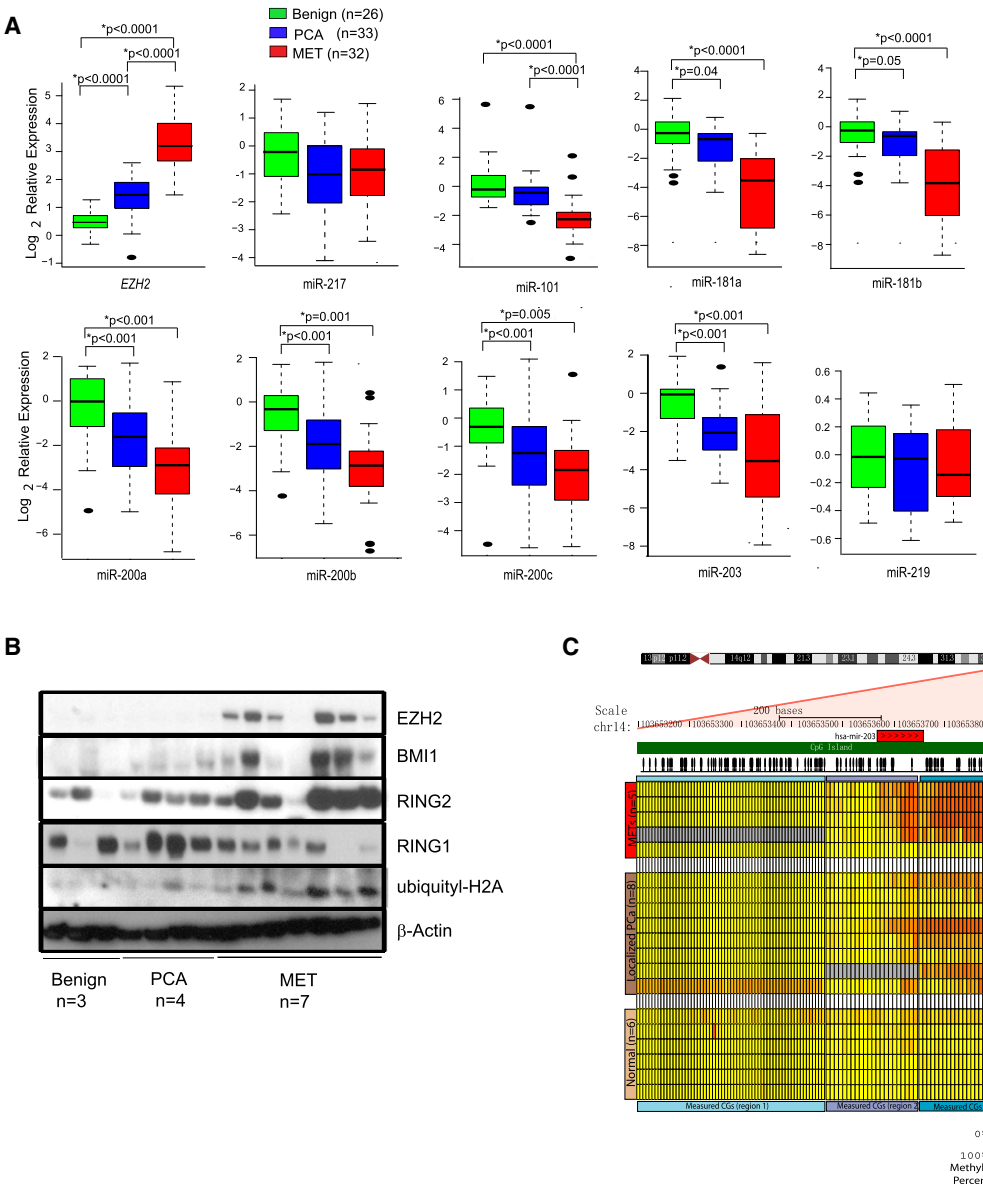


**Figure 6. Coordinated Expression of PcG Proteins and PRC Regulatory miRNAs in Prostate Cancer Progression**

(A) Expression of indicated miRs as assessed by q-PCR in benign prostate, clinically localized prostate cancer and metastatic prostate cancer tissues. Data for EZH2, miR-217, and miR-101 were reported previously (Varambally et al., 2008) and displayed here for comparison (Student's t test).

(B) Immunoblot analysis of EZH2, BMI-1, RING2, RING1, and ubiquityl-H2A in benign prostate, clinically localized prostate cancer, and metastatic prostate cancer.

(C) Bisulfite sequencing analysis of the miR-203 genomic region revealed cancer-specific DNA methylation in a region proximal to miR-203 in prostate cancer tissues.

All bar graphs are shown with ± SEM. See also Figure S6.

regulates PRC2 protein SUZ12 in a manner similar to that of miR-101, lending further support for microRNA-mediated PRC activity during cancer progression. These findings offer multiple targets for therapeutic interventions in the treatment of aggressive cancers (Garzon et al., 2010).

## EXPERIMENTAL PROCEDURES

### Cell Lines

Breast cancer cell line BT-549 was grown in RPMI 1640 (Invitrogen, Carlsbad, CA) with 0.023 IU/ml insulin and 10% FBS (Invitrogen) in 5% $CO_2$ cell culture incubator; breast cancer cell line SKBr3 was grown in RPMI 1640 (Invitrogen) with 10% FBS (Invitrogen) in 5% $CO_2$ cell culture incubator; and prostate cancer cell line DU145 was grown in MEM with 10% FBS in 5% $CO_2$ cell culture incubator. Immortalized breast cell lines HME and H16N2 were grown in F-12 Nutrient Mixture with 5μg/ml Insulin (Sigma, St. Louis, MO), 1 μg/ml Hydrocortisone (Sigma), 10 ng/ml EGF (Invitrogen), 5 mM Ethanolamine (Sigma), 5 μg/ml Transferrin (Sigma), 10 nM Triiodo Thyronine (Sigma), 50 nM Sodium Selenite (Sigma), 10 mM HEPES (Invitrogen) and 50 unit/ml Penstrep (Invitrogen), 10% $CO_2$. The PrEC (Lonza, Conshohocken, PA) and RWPE (ATCC, Manassas, VA) cells were grown in their respective medium as specified by the suppliers. miR-181b, miR-200b, and miR-203 overexpression constructs were obtained from Openbiosystems (Huntsville, AL).

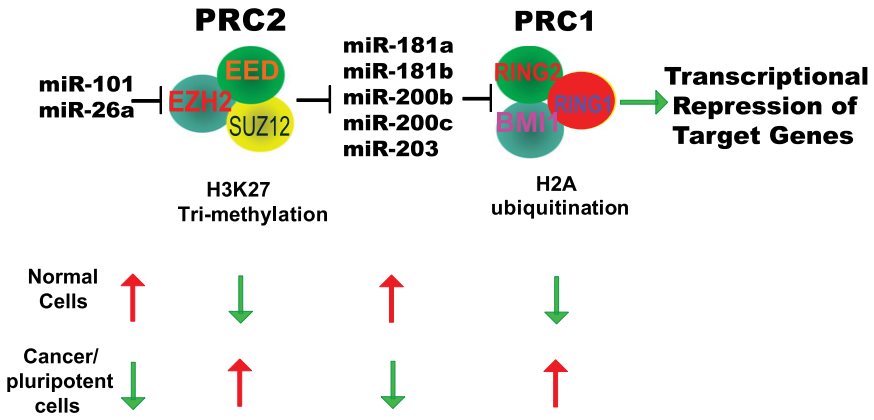


**Figure 7. A Proposed Model Role for microRNAs in Regulating PRCs**
Specifically, PRC2 is molecularly linked to PRC1 via a set of regulatory miRs.

Lentiviruses were generated by the University of Michigan Vector Core. BMI1, RING2 and control shRNA lentivirus were obtain from Sigma. Prostate cancer cell line DU145 was infected with lentiviruses expressing BMI1 shRNA, RING2 shRNA, miR-181b, miR-200b, and miR-203 or controls only, and stable cell lines were generated by selection with 300 μg/ml puromycin (Invitrogen).

### Benign and Tumor Tissues

In this study, we utilized tissues from clinically localized prostate cancer patients who underwent radical prostatectomy as a primary therapy between 2004 and 2006 at the University of Michigan Hospital. Samples were also used from androgen-independent metastatic prostate cancer patients from a rapid autopsy program described previously (Tomlins et al., 2005, 2007a). The detailed clinical and pathological data are maintained in a secure relational database. This study was approved by the Institutional Review Board at the University of Michigan Medical School. Informed consent was also obtained from all subjects through the Institutional Review Board at the University of Michigan Medical School. Both radical prostatectomy series and the rapid autopsy program are part of the University of Michigan Prostate Cancer Specialized Program of Research Excellence Tissue Core.

### Illumina microRNA Profiling

Total RNA (500 ng) from each sample was labeled and hybridized on the Human v2 microRNA Expression BeadChips (Illumina, San Diego, CA) according to the manufacturers recommendations. BeadChips were scanned with the Illumina iScan Reader. Data were then average median normalized before generating differential expression values between treated and control samples.

### microRNA Transfection, AntagomiR Transfection, and Small RNA Interference

Knockdown of EZH2 or Dicer was accomplished by RNA interference using siRNA duplexes (Dharmacon, Lafayette, CO) as previously described (Varambally et al., 2002). Precursors of respective microRNAs, antagomiRs and negative controls were purchased from Ambion (Austin, TX). Transfections were performed with oligofectamine (Invitrogen). EZH2 siRNA duplexes sequences, (duplex 1: GAGGTTCAGACGAGCTGAT; duplex 2: AGACTCT GAATGCA GTTGC).

### miR Reporter Luciferase Assays

The 50 bp of wild-type or mutant 3′ UTR of BMI1 and RING2 containing the predicted miR-181a,b, miR-200b,c or miR-203 binding sites (as described in Figures S2C–S2F) were cloned into the pMIR-REPORT miRNA Expression Reporter Vector (Ambion). BT-549 cells were transfected with miRNAs or controls and then cotransfected with wild-type 3′ UTR-luc or mutant 3′ UTR-luc, as well as pRL-TK vector as internal control for luciferase activity. After 48 hours of transfection, the cells were lysed and luciferase assays were conducted using the dual luciferase assay system (Promega, Madison, WI). Each experiment was performed in triplicate. Drug Treatment.

BT-549 and DU145 cells were treated with 5 μM 5-aza-2′-deoxycytidine (5-aza-dC) for 6 days (fresh media change containing the drug was performed every other day) and/or 1μM suberoylanilide hydroxamic acid (SAHA) for 2 days. DU145 cells were treated with 2.5 or 5 μM deazaneplanocin A (DZNep) for 2 or 3 days followed by RNA extraction or chromatin immunoprecipitation.

### Cell Proliferation Assay and Basement Membrane Matrix Invasion Assays

Invasive breast cancer cell BT-549 and prostate cancer cell DU145 were transfected with miRNAs or controls. The cell proliferation and invasion assays were performed as described (Cao et al., 2008; Kleer et al., 2003; Varambally et al., 2008; Yu et al., 2007b).

### Soft Agar Colony Formation Assays

A 50 μl base layer of agar (0.6% Agar in DMEM with 10% FBS) was allowed to solidify in a 96-well flat-bottom plate prior to the addition of a 75 μl miRNAs or control-transfected or stable DU145 cell suspension containing 4000 cells in 0.4% Agar in DMEM with 10% FBS. The cell containing layer was then solidified at 4C for 15 min prior to the addition of 100 μl of MEM with 5% FBS. Colonies were allowed to grow for 21 days followed by counting and imaging under a light microscope.

### Spheres Culture

Spheres culture was performed as described (Dontu et al., 2003; Yu et al., 2007a). Briefly, cells (1000 cells/ml) were cultured in suspension in serum-free DMEM-F12 (Invitrogen), supplemented with B27 (1:50, Invitrogen), 20 ng/ml EGF (BD Biosciences), 0.4% bovine serum albumin (Sigma), and 4 μg/ml insulin (Sigma). To propagate spheres in vitro, spheres were collected by gentle centrifugation, dissociated to single cells as described (Dontu et al., 2003; Yu et al., 2007a), and then cultured to generate prostatospheres of the next generation. Spheres larger than 50 μm were counted.

### Gene Expression Profiling

Expression profiling was performed using the Agilent Whole Human Genome Oligo Microarray (Santa Clara, CA) according to the manufacturer's protocol. BT-549 and DU145 cells were transfected with miRNAs or negative control for precursor microRNA. Over- and underexpressed signatures were generated by filtering to include only features with significant differential expression (Log ratio, $p < .01$) in all hybridizations and 2-fold average over- or under-expression (Log ratio). Gene expression data are deposited into GEO (GSE26996).

### Gene Set Enrichment Analysis

Molecular Concept Map (MCM) analysis was performed using gene list of putative targets to search for all concepts available in the Oncomine database as previously described (Yu et al., 2007c). Representative concepts with significant enrichment ($p < 0.001$) were displayed as a network (Figure 4G; Table S4).

### Prostate Tumor Xenograft Model

All procedures involving mice were approved by the University Committee on Use and Care of Animals (UCUCA) at the University of Michigan and conform to their relevant regulatory standards. Five-week-old male nude athymic BALB/c nu/nu mice (Charles River Laboratory, Wilmington, MA) were used for examining tumorigenicity. To evaluate the role of BMI1 and RING2 knockdown, or miR-181b, miR-200b, and miR-203 overexpression in tumor formation, the DU145 stably overexpressing BMI1 shRNA, RING2 shRNA, scramble shRNA, miR-181b, miR-200b, miR-203, nontargeting miR or vector control cells were propagated and $5 \times 10^6$ cells were inoculated subcutaneously into the dorsal flank of mice (n = 7 for miR-203, n = 9 for vector control, and n = 8 for Scramble, BMI1-sh3, RING2-sh1, miR-181b, miR-200b, and miR-NT,

respectively). Tumor size was measured every week, and tumor volumes were estimated using the formula $(\pi/6)$ $(L \times W^2)$, where $L$ = length of tumor and $W$ = width.

### Bisulfite Modification and Methylation-Specific PCR of miR-203 in Prostate Tissues

Bisulfite conversion was carried out using EZ DNA methylation gold kit (Zymo Research Corporation, Orange, CA) according to manufacturer's instructions. Purified DNA (2 μl) was used as template for PCRs with primers (Integrated DNA Technologies Inc., San Diego, CA) and synthesized according to bisulfite converted DNA sequences for the regions of interest using the Methprimer software (Li and Dahiya, 2002). The PCR product was gel purified and cloned into pCR4 TOPO TA sequencing vector (Invitrogen, Carlsbad, CA). Plasmid DNA isolated from ten colonies from each sample was sequenced by conventional Sanger Sequencing (University of Michigan DNA Sequencing Core). The "BIQ Analyzer" (Bock et al., 2005) online tool was used to calculate the methylation percentage and to generate the bar graphs.

## ACCESSION NUMBERS

Coordinates have been deposited in Gene Expression Omnibus database with accession code GSE26996.

## SUPPLEMENTAL INFORMATION

Supplemental Information includes six figures, four tables, and Supplemental Experimental Procedures and can be found with this article online at doi:10.1016/j.ccr.2011.06.016.

## ACKNOWLEDGMENTS

We thank Xia Jiang, Javed Siddiqui, Wei Yan, Bo Han, Khalid Suleman, Rohit Mehra, Rupal Shastri, and Joy E. Tsai for technical assistance, Victor E. Marquez for providing DZNep, Michigan Center for hES Cell Research for H7 RNA and qPCR, the University of Michigan Vector Core for generating adenovirus and lentivirus, Kenneth J. Pienta, Xiaosong Wang, and Shanker Kalyana-Sundaram for discussions, and Jyoti Athanikar and Karen Giles for critically reading the manuscript and submission documents. This work is supported in part by the Early Detection Research Network UO1 CA111275, Prostate SPORE P50CA69568 and P50CA090386, and National Institutes of Health (R01CA132874, R01CA157845). A.M.C. is supported by the Doris Duke Charitable Foundation Clinical Scientist Award, Burroughs Welcome Foundation Award in Clinical Translational Research, the Prostate Cancer Foundation (PCF) and the Howard Hughes Medical Institute. A.M.C. is an American Cancer Society Research Professor. Q.C., J.R.P., and J.C.B. are supported by U.S. Department of Defense (PC094725 to Q.C.; PC094290 to J.R.P.; BC083217 to J.C.B.); R.-S.M., S.A.T., and C.A.M. are supported by Young Investigator Awards from the PCF; B.A. is supported by the Genentech Foundation Postdoctoral Fellowship and Young Investigator Award from the Expedition Inspiration Fund for Breast Cancer Research. N.P. is supported by the University of Michigan Prostate Cancer SPORE Career Development award. Z.Q. is supported by National Institutes of Health (7R01HG005119-02). J.Y. is supported by U.S. Department of Defense (PC080665) and National Institutes of Health (5R00CA129565); S.V. is supported by National Institutes of Health (R01CA157845) and Prostate Cancer SPORE Career Development award. Q.C. and A.M.C. designed the experiments. Q.C., R.-S.M., B.A., S.M.D., I.A.A., J.R.P., J.H.K., J.C.B., X.J., X.C., R.W., Y.L., A.D., L.W., M.P., Y.-M.W., S.A.T., N.P., J.Y., and S.V. performed the experimental work. R.J.L., Z.Q., and C.A.M. performed statistical analysis on miRNA and gene expression data. Q.C. and A.M.C. wrote the paper. All authors discussed the results and commented on the manuscript.

Received: January 31, 2011
Revised: May 18, 2011
Accepted: June 17, 2011
Published: August 15, 2011

## REFERENCES

Bock, C., Reither, S., Mikeska, T., Paulsen, M., Walter, J., and Lengauer, T. (2005). BiQ Analyzer: visualization and quality control for DNA methylation data from bisulfite sequencing. Bioinformatics *21*, 4067–4068.

Bonci, D., Coppola, V., Musumeci, M., Addario, A., Giuffrida, R., Memeo, L., D'Urso, L., Pagliuca, A., Biffoni, M., Labbaye, C., et al. (2008). The miR-15a-miR-16-1 cluster controls prostate cancer by targeting multiple oncogenic activities. Nat. Med. *14*, 1271–1277.

Bracken, A.P., and Helin, K. (2009). Polycomb group proteins: navigators of lineage pathways led astray in cancer. Nature Rev. *9*, 773–784.

Bracken, A.P., Pasini, D., Capra, M., Prosperini, E., Colli, E., and Helin, K. (2003). EZH2 is downstream of the pRB-E2F pathway, essential for proliferation and amplified in cancer. EMBO J. *22*, 5323–5335.

Cao, R., Wang, L., Wang, H., Xia, L., Erdjument-Bromage, H., Tempst, P., Jones, R.S., and Zhang, Y. (2002). Role of histone H3 lysine 27 methylation in Polycomb-group silencing. Science *298*, 1039–1043.

Cao, R., Tsukada, Y., and Zhang, Y. (2005). Role of Bmi-1 and Ring1A in H2A ubiquitylation and Hox gene silencing. Mol. Cell *20*, 845–854.

Cao, Q., Yu, J., Dhanasekaran, S.M., Kim, J.H., Mani, R.S., Tomlins, S.A., Mehra, R., Laxman, B., Cao, X., Yu, J., et al. (2008). Repression of E-cadherin by the polycomb group protein EZH2 in cancer. Oncogene *27*, 7274–7284.

Cao, P., Deng, Z., Wan, M., Huang, W., Cramer, S.D., Xu, J., Lei, M., and Sui, G. (2010). MicroRNA-101 negatively regulates Ezh2 and its expression is modulated by androgen receptor and HIF-1alpha/HIF-1beta. Mol. Cancer *9*, 108.

Chen, H., Tu, S.W., and Hsieh, J.T. (2005). Down-regulation of human DAB2IP gene expression mediated by polycomb Ezh2 complex and histone deacetylase in prostate cancer. J. Biol. Chem. *280*, 22437–22444.

Chiang, C.W., Huang, Y., Leong, K.W., Chen, L.C., Chen, H.C., Chen, S.J., and Chou, C.K. (2010). PKCalpha mediated induction of miR-101 in human hepatoma HepG2 cells. J. Biomed. Sci. *17*, 35.

Dontu, G., Abdallah, W.M., Foley, J.M., Jackson, K.W., Clarke, M.F., Kawamura, M.J., and Wicha, M.S. (2003). In vitro propagation and transcriptional profiling of human mammary stem/progenitor cells. Genes Dev. *17*, 1253–1270.

Ezhkova, E., Pasolli, H.A., Parker, J.S., Stokes, N., Su, I.H., Hannon, G., Tarakhovsky, A., and Fuchs, E. (2009). Ezh2 orchestrates gene expression for the stepwise differentiation of tissue-specific stem cells. Cell *136*, 1122–1135.

Faber, J., Gregory, R.I., and Armstrong, S.A. (2008). Linking miRNA regulation to BCR-ABL expression: the next dimension. Cancer Cell *13*, 467–469.

Fasano, C.A., Dimos, J.T., Ivanova, N.B., Lowry, N., Lemischka, I.R., and Temple, S. (2007). shRNA knockdown of Bmi-1 reveals a critical role for p21-Rb pathway in NSC self-renewal during development. Cell Stem Cell *1*, 87–99.

Friedman, J.M., Liang, G., Liu, C.C., Wolff, E.M., Tsai, Y.C., Ye, W., Zhou, X., and Jones, P.A. (2009). The putative tumor suppressor microRNA-101 modulates the cancer epigenome by repressing the polycomb group protein EZH2. Cancer Res. *69*, 2623–2629.

Fujii, S., Ito, K., Ito, Y., and Ochiai, A. (2008). Enhancer of zeste homologue 2 (EZH2) down-regulates RUNX3 by increasing histone H3 methylation. J. Biol. Chem. *283*, 17324–17332.

Galmozzi, E., Facchetti, F., and La Porta, C.A. (2006). Cancer stem cells and therapeutic perspectives. Curr. Med. Chem. *13*, 603–607.

Garzon, R., Marcucci, G., and Croce, C.M. (2010). Targeting microRNAs in cancer: rationale, strategies and challenges. Nat. Rev. Drug Discov. *9*, 775–789.

Glinsky, G.V., Berezovska, O., and Glinskii, A.B. (2005). Microarray analysis identifies a death-from-cancer signature predicting therapy failure in patients with multiple types of cancer. J. Clin. Invest. *115*, 1503–1521.

Gupta, R.A., Shah, N., Wang, K.C., Kim, J., Horlings, H.M., Wong, D.J., Tsai, M.C., Hung, T., Argani, P., Rinn, J.L., et al. (2010). Long non-coding RNA

HOTAIR reprograms chromatin state to promote cancer metastasis. Nature *464*, 1071–1076.

Hurt, E.M., Kawasaki, B.T., Klarmann, G.J., Thomas, S.B., and Farrar, W.L. (2008). CD44+ CD24(-) prostate cells are early cancer progenitor/stem cells that provide a model for patients with poor prognosis. Br. J. Cancer *98*, 756–765.

Iliopoulos, D., Lindahl-Allen, M., Polytarchou, C., Hirsch, H.A., Tsichlis, P.N., and Struhl, K. (2010). Loss of miR-200 inhibition of Suz12 leads to polycomb-mediated repression required for the formation and maintenance of cancer stem cells. Mol. Cell *39*, 761–772.

Jacobs, J.J., Kieboom, K., Marino, S., DePinho, R.A., and van Lohuizen, M. (1999a). The oncogene and Polycomb-group gene bmi-1 regulates cell proliferation and senescence through the ink4a locus. Nature *397*, 164–168.

Jacobs, J.J., Scheijen, B., Voncken, J.W., Kieboom, K., Berns, A., and van Lohuizen, M. (1999b). Bmi-1 collaborates with c-Myc in tumorigenesis by inhibiting c-Myc-induced apoptosis via INK4a/ARF. Genes Dev. *13*, 2678–2690.

Johnson, S.M., Grosshans, H., Shingara, J., Byrom, M., Jarvis, R., Cheng, A., Labourier, E., Reinert, K.L., Brown, D., and Slack, F.J. (2005). RAS is regulated by the let-7 microRNA family. Cell *120*, 635–647.

Kaneko, S., Li, G., Son, J., Xu, C.F., Margueron, R., Neubert, T.A., and Reinberg, D. (2010). Phosphorylation of the PRC2 component Ezh2 is cell cycle-regulated and up-regulates its binding to ncRNA. Genes Dev. *24*, 2615–2620.

Kleer, C.G., Cao, Q., Varambally, S., Shen, R., Ota, I., Tomlins, S.A., Ghosh, D., Sewalt, R.G., Otte, A.P., Hayes, D.F., et al. (2003). EZH2 is a marker of aggressive breast cancer and promotes neoplastic transformation of breast epithelial cells. Proc. Natl. Acad. Sci. USA *100*, 11606–11611.

Krützfeldt, J., Rajewsky, N., Braich, R., Rajeev, K.G., Tuschl, T., Manoharan, M., and Stoffel, M. (2005). Silencing of microRNAs in vivo with "antagomirs". Nature *438*, 685–689.

Lawson, D.A., Xin, L., Lukacs, R.U., Cheng, D., and Witte, O.N. (2007). Isolation and functional characterization of murine prostate stem cells. Proc. Natl. Acad. Sci. USA *104*, 181–186.

Li, L.C., and Dahiya, R. (2002). MethPrimer: designing primers for methylation PCRs. Bioinformatics *18*, 1427–1431.

Lu, J., He, M.L., Wang, L., Chen, Y., Liu, X., Dong, Q., Chen, Y.C., Peng, Y., Yao, K.T., Kung, H.F., and Li, X.P. (2011). MiR-26a inhibits cell growth and tumorigenesis of nasopharyngeal carcinoma through repression of EZH2. Cancer Res. *71*, 225–233.

Lukacs, R.U., Memarzadeh, S., Wu, H., and Witte, O.N. (2010). Bmi-1 is a crucial regulator of prostate stem cell self-renewal and malignant transformation. Cell Stem Cell *7*, 682–693.

Margueron, R., and Reinberg, D. (2011). The Polycomb complex PRC2 and its mark in life. Nature *469*, 343–349.

Matsukawa, Y., Semba, S., Kato, H., Ito, A., Yanagihara, K., and Yokozaki, H. (2006). Expression of the enhancer of zeste homolog 2 is correlated with poor prognosis in human gastric cancer. Cancer Sci. *97*, 484–491.

Min, J., Zaslavsky, A., Fedele, G., McLaughlin, S.K., Reczek, E.E., De Raedt, T., Guney, I., Strochlic, D.E., Macconaill, L.E., Beroukhim, R., et al. (2010). An oncogene-tumor suppressor cascade drives metastatic prostate cancer by coordinately activating Ras and nuclear factor-kappaB. Nat. Med. *16*, 286–294.

Palanisamy, N., Ateeq, B., Kalyana-Sundaram, S., Pflueger, D., Ramnarayanan, K., Shankar, S., Han, B., Cao, Q., Cao, X., Suleman, K., et al. (2010). Rearrangements of the RAF kinase pathway in prostate cancer, gastric cancer and melanoma. Nat. Med. *16*, 793–798.

Park, S.M., Gaur, A.B., Lengyel, E., and Peter, M.E. (2008). The miR-200 family determines the epithelial phenotype of cancer cells by targeting the E-cadherin repressors ZEB1 and ZEB2. Genes Dev. *22*, 894–907.

Pereira, C.F., Piccolo, F.M., Tsubouchi, T., Sauer, S., Ryan, N.K., Bruno, L., Landeira, D., Santos, J., Banito, A., Gil, J., et al. (2010). ESCs require PRC2 to direct the successful reprogramming of differentiated cells toward pluripotency. Cell Stem Cell *6*, 547–556.

Pietersen, A.M., Evers, B., Prasad, A.A., Tanger, E., Cornelissen-Steijger, P., Jonkers, J., and van Lohuizen, M. (2008). Bmi1 regulates stem cells and proliferation and differentiation of committed cells in mammary epithelium. Curr. Biol. *18*, 1094–1099.

Poliseno, L., Salmena, L., Riccardi, L., Fornari, A., Song, M.S., Hobbs, R.M., Sportoletti, P., Varmeh, S., Egia, A., Fedele, G., et al. (2010). Identification of the miR-106b~25 microRNA cluster as a proto-oncogenic PTEN-targeting intron that cooperates with its host gene MCM7 in transformation. Sci. Signal. *3*, ra29.

Rinn, J.L., Kertesz, M., Wang, J.K., Squazzo, S.L., Xu, X., Brugmann, S.A., Goodnough, L.H., Helms, J.A., Farnham, P.J., Segal, E., and Chang, H.Y. (2007). Functional demarcation of active and silent chromatin domains in human HOX loci by noncoding RNAs. Cell *129*, 1311–1323.

Sánchez-Beato, M., Sánchez, E., González-Carreró, J., Morente, M., Díez, A., Sánchez-Verde, L., Martín, M.C., Cigudosa, J.C., Vidal, M., and Piris, M.A. (2006). Variability in the expression of polycomb proteins in different normal and tumoral tissues. A pilot study using tissue microarrays. Mod. Pathol. *19*, 684–694.

Shimono, Y., Zabala, M., Cho, R.W., Lobo, N., Dalerba, P., Qian, D., Diehn, M., Liu, H., Panula, S.P., Chiao, E., et al. (2009). Downregulation of miRNA-200c links breast cancer stem cells with normal stem cells. Cell *138*, 592–603.

Sudo, T., Utsunomiya, T., Mimori, K., Nagahara, H., Ogawa, K., Inoue, H., Wakiyama, S., Fujita, H., Shirouzu, K., and Mori, M. (2005). Clinicopathological significance of EZH2 mRNA expression in patients with hepatocellular carcinoma. Br. J. Cancer *92*, 1754–1758.

Surface, L.E., Thornton, S.R., and Boyer, L.A. (2010). Polycomb group proteins set the stage for early lineage commitment. Cell Stem Cell *7*, 288–298.

Tan, J., Yang, X., Zhuang, L., Jiang, X., Chen, W., Lee, P.L., Karuturi, R.K., Tan, P.B., Liu, E.T., and Yu, Q. (2007). Pharmacologic disruption of Polycomb-repressive complex 2-mediated gene repression selectively induces apoptosis in cancer cells. Genes Dev. *21*, 1050–1063.

Tomlins, S.A., Rhodes, D.R., Perner, S., Dhanasekaran, S.M., Mehra, R., Sun, X.W., Varambally, S., Cao, X., Tchinda, J., Kuefer, R., et al. (2005). Recurrent fusion of TMPRSS2 and ETS transcription factor genes in prostate cancer. Science *310*, 644–648.

Tomlins, S.A., Laxman, B., Dhanasekaran, S.M., Helgeson, B.E., Cao, X., Morris, D.S., Menon, A., Jing, X., Cao, Q., Han, B., et al. (2007a). Distinct classes of chromosomal rearrangements create oncogenic ETS gene fusions in prostate cancer. Nature *448*, 595–599.

Tomlins, S.A., Mehra, R., Rhodes, D.R., Cao, X., Wang, L., Dhanasekaran, S.M., Kalyana-Sundaram, S., Wei, J.T., Rubin, M.A., Pienta, K.J., et al. (2007b). Integrative molecular concept modeling of prostate cancer progression. Nat. Genet. *39*, 41–51.

Valk-Lingbeek, M.E., Bruggeman, S.W., and van Lohuizen, M. (2004). Stem cells and cancer; the polycomb connection. Cell *118*, 409–418.

Varambally, S., Dhanasekaran, S.M., Zhou, M., Barrette, T.R., Kumar-Sinha, C., Sanda, M.G., Ghosh, D., Pienta, K.J., Sewalt, R.G., Otte, A.P., et al. (2002). The polycomb group protein EZH2 is involved in progression of prostate cancer. Nature *419*, 624–629.

Varambally, S., Yu, J., Laxman, B., Rhodes, D.R., Mehra, R., Tomlins, S.A., Shah, R.B., Chandran, U., Monzon, F.A., Becich, M.J., et al. (2005). Integrative genomic and proteomic analysis of prostate cancer reveals signatures of metastatic progression. Cancer Cell *8*, 393–406.

Varambally, S., Cao, Q., Mani, R.S., Shankar, S., Wang, X., Ateeq, B., Laxman, B., Cao, X., Jing, X., Ramnarayanan, K., et al. (2008). Genomic loss of microRNA-101 leads to overexpression of histone methyltransferase EZH2 in cancer. Science *322*, 1695–1699.

Viré, E., Brenner, C., Deplus, R., Blanchon, L., Fraga, M., Didelot, C., Morey, L., Van Eynde, A., Bernard, D., Vanderwinden, J.M., et al. (2006). The Polycomb group protein EZH2 directly controls DNA methylation. Nature *439*, 871–874.

Wang, H., Wang, L., Erdjument-Bromage, H., Vidal, M., Tempst, P., Jones, R.S., and Zhang, Y. (2004). Role of histone H2A ubiquitination in Polycomb silencing. Nature *431*, 873–878.

Wang, H.J., Ruan, H.J., He, X.J., Ma, Y.Y., Jiang, X.T., Xia, Y.J., Ye, Z.Y., and Tao, H.Q. (2010). MicroRNA-101 is down-regulated in gastric cancer and involved in cell migration and invasion. Eur. J. Cancer *46*, 2295–2303.

Wang, X.-S., Shanka, S., Dhanasekaran, S.M., Ateeq, B., Sasaki, A.T., Jing, X., Robinson, D., Cao, Q., Prensner, J.R., Yocum, A.K., et al. (2011). Characterization of KRAS rearrangements in metastatic prostate cancer. Cancer Discovery *1*. Published online April 3, 2011. 10.1158/2159-8274.CD-10-0022.

Wellner, U., Schubert, J., Burk, U.C., Schmalhofer, O., Zhu, F., Sonntag, A., Waldvogel, B., Vannier, C., Darling, D., zur Hausen, A., et al. (2009). The EMT-activator ZEB1 promotes tumorigenicity by repressing stemness-inhibiting microRNAs. Nat. Cell Biol. *11*, 1487–1495.

Wong, C.F., and Tellam, R.L. (2008). MicroRNA-26a targets the histone methyltransferase Enhancer of Zeste homolog 2 during myogenesis. J. Biol. Chem. *283*, 9836–9843.

Yi, R., Poy, M.N., Stoffel, M., and Fuchs, E. (2008). A skin microRNA promotes differentiation by repressing "stemness". Nature *452*, 225–229.

Yu, F., Yao, H., Zhu, P., Zhang, X., Pan, Q., Gong, C., Huang, Y., Hu, X., Su, F., Lieberman, J., and Song, E. (2007a). let-7 regulates self renewal and tumorigenicity of breast cancer cells. Cell *131*, 1109–1123.

Yu, J., Cao, Q., Mehra, R., Laxman, B., Yu, J., Tomlins, S.A., Creighton, C.J., Dhanasekaran, S.M., Shen, R., Chen, G., et al. (2007b). Integrative genomics analysis reveals silencing of beta-adrenergic signaling by polycomb in prostate cancer. Cancer Cell *12*, 419–431.

Yu, J., Yu, J., Rhodes, D.R., Tomlins, S.A., Cao, X., Chen, G., Mehra, R., Wang, X., Ghosh, D., Shah, R.B., et al. (2007c). A polycomb repression signature in metastatic prostate cancer predicts cancer outcome. Cancer Res. *67*, 10657–10663.

Yu, J., Cao, Q., Yu, J., Wu, L., Dallol, A., Li, J., Chen, G., Grasso, C., Cao, X., Lonigro, R.J., et al. (2010). The neuronal repellent SLIT2 is a target for repression by EZH2 in prostate cancer. Oncogene *29*, 5370–5380.